



This discussion paper is/has been under review for the journal Atmospheric Measurement Techniques (AMT). Please refer to the corresponding final paper in AMT if available.

Diode laser-based cavity ring-down instrument for NO_3 , N_2O_5 , NO , NO_2 and O_3 from aircraft

N. L. Wagner^{1,2}, W. P. Dubé^{1,2}, R. A. Washenfelder^{1,2}, C. J. Young^{1,2}, I. B. Pollack^{1,2}, T. B. Ryerson¹, and S. S. Brown¹

¹NOAA Earth System Research Laboratory, R/CSD7, 325 Broadway, Boulder, CO 80305, USA

²Cooperative Institute for Research in Environmental Sciences, University of Colorado, Boulder, CO 80309, USA

Received: 9 February 2011 – Accepted: 14 February 2011 – Published: 3 March 2011

Correspondence to: S. S. Brown (steven.s.brown@noaa.gov)

Published by Copernicus Publications on behalf of the European Geosciences Union.

AMTD

4, 1555–1591, 2011

Cavity ring-down instrument for N_2O_5 , NO , NO_2 and O_3

N. L. Wagner et al.

Title Page

Abstract

Introduction

Conclusions

References

Tables

Figures

◀

▶

◀

▶

Back

Close

Full Screen / Esc

Printer-friendly Version

Interactive Discussion



Abstract

This article presents a diode laser based, cavity ring-down spectrometer for simultaneous in situ measurements of four nitrogen oxide species, NO_3 , N_2O_5 , NO , NO_2 , as well as O_3 , designed for deployment on aircraft. The instrument measures NO_3 and NO_2 by optical extinction at 662 nm and 405 nm, respectively; N_2O_5 is measured by thermal conversion to NO_3 , while NO and O_3 are measured by chemical conversion to NO_2 . The instrument has several advantages over previous instruments developed by our group for measurement of NO_2 , NO_3 and N_2O_5 alone, based on a pulsed Nd:YAG and dye laser. First, the use of continuous wave diode lasers reduces the requirements for power and weight and eliminates hazardous materials. Second, detection of NO_2 at 405 nm is more sensitive than our previously reported 532 nm instrument, and does not have a measurable interference from O_3 . Third, the instrument includes chemical conversion of NO and O_3 to NO_2 to provide measurements of total NO_x ($= \text{NO} + \text{NO}_2$) and O_x ($= \text{NO}_2 + \text{O}_3$) on two separate channels; mixing ratios of NO and O_3 are determined by subtraction of NO_2 . Finally, all five species are calibrated against a single standard based on 254 nm O_3 absorption to provide high accuracy. Disadvantages include an increased sensitivity to water vapor on the 662 nm NO_3 and N_2O_5 channels and a modest reduction in sensitivity for these species compared to the pulsed laser instrument. The measurement precision for both NO_3 and N_2O_5 is below 1 pptv (2σ , 1 s) and for NO , NO_2 and O_3 is 170, 46, and 56 pptv (2σ , 1 s) respectively. The NO and NO_2 measurements are less precise than research-grade chemiluminescence instruments. However, the combination of these five species in a single instrument, calibrated to a single analytical standard, provides a complete and accurate picture of nighttime nitrogen oxide chemistry. The instrument performance is demonstrated using data acquired during a recent field campaign in California.

AMTD

4, 1555–1591, 2011

Cavity ring-down instrument for N_2O_5 , NO , NO_2 and O_3

N. L. Wagner et al.

[Title Page](#)

[Abstract](#)

[Introduction](#)

[Conclusions](#)

[References](#)

[Tables](#)

[Figures](#)

◀

▶

◀

▶

[Back](#)

[Close](#)

[Full Screen / Esc](#)

[Printer-friendly Version](#)

[Interactive Discussion](#)



1 Introduction

The nitrate radical, NO_3 and its reservoir species, dinitrogen pentoxide (N_2O_5) are important trace gases in the nocturnal atmosphere (Wayne et al., 1991). NO_3 is formed by reaction of ozone with NO_2 (Reaction R1), and NO_3 then reacts with NO_2 to reversibly form N_2O_5 (Reaction R2).



These species are typically present at very modest levels during daytime because NO_3 undergoes rapid photolysis and reaction with NO, which is present during the day and in close proximity to large NO_x emission sources during the night.



The nitrate radical is a strong oxidant and is consumed by reactions with biogenic VOCs and sulfur compounds, and some classes of highly reactive anthropogenic VOCs (Atkinson, 1991). N_2O_5 undergoes heterogeneous uptake to aerosol. Its hydrolysis leads either to non-photochemical conversion of NO_x to soluble nitrate via production of HNO_3 (Jones and Seinfeld, 1983), or to activation of photolabile halogens through formation of nitryl chloride, ClNO_2 (Finlayson-Pitts et al., 1989; Thornton et al., 2010). Thus, NO_3 and N_2O_5 are intermediates in a number of important atmospheric chemical transformations, and understanding their atmospheric concentrations is an important topic of current research.

Much of the prior database for understanding these processes was based on measurements of NO_3 by differential optical absorption spectroscopy (DOAS) over a long, open path or by passive techniques using natural light sources (Platt et al., 1980;

Title Page

Abstract

Introduction

Conclusions

References

Tables

Figures

◀

▶

Back

Close

Full Screen / Esc

Printer-friendly Version

Interactive Discussion



Solomon et al., 1989; Plane and Nien, 1992). Such measurements have been extremely useful in developing an understanding of the factors that govern nighttime chemistry. In situ instruments add to this database by enabling measurements from mobile platforms, such as aircraft and ships (e.g., Brown et al., 2007a), and from tall towers (e.g., Brown et al., 2007b). The in situ measurements are valuable for characterizing the strong vertical gradients characteristic of the nocturnal boundary layer or for measurements within the residual daytime boundary layer.

Cavity ring-down spectroscopy (CRDS) is a sensitive technique for in situ measurement of atmospheric trace gases (Brown, 2003). In situ measurement of NO_3 was first developed approximately a decade ago and was based on CRDS with either a pulsed dye laser (Brown et al., 2002) or extended cavity diode laser (King et al., 2000). Thermal conversion of N_2O_5 to NO_3 in a second channel enabled direct measurement of the sum of the two compounds and measurement of N_2O_5 itself by difference. This development ultimately led to the deployment of a CRDS instrument for NO_3 and N_2O_5 on aircraft (Dubé et al., 2006). Although the pulsed laser system used in this instrument had a relatively small footprint, such laser systems are in general somewhat cumbersome for field instruments because of their requirements for power and weight. In addition, the use of toxic dyes and solvents requires hazardous materials that are not ideal for field environments, especially aircraft.

The aircraft instrument described above also incorporated measurements of NO_2 by pulsed laser CRDS at 532 nm by taking advantage of the Nd:YAG laser second harmonic that was used to pump the dye laser (Osthoff et al., 2006). These NO_2 measurements required active subtraction of an interference from ozone, but were otherwise accurate (Fuchs et al., 2010). These CRDS NO_2 measurements have recently been further developed using a diode laser with a center wavelength near 405 nm (Fuchs et al., 2009). Because there is no significant interference from ozone at this wavelength, this approach is capable of simultaneous detection of NO via its conversion to NO_2 in excess ozone. We have also recently demonstrated the analogous conversion of O_3 to NO_2 in excess NO (Washenfelder et al., 2011).

Cavity ring-down instrument for N_2O_5 , NO , NO_2 and O_3

N. L. Wagner et al.

[Title Page](#)

[Abstract](#)

[Introduction](#)

[Conclusions](#)

[References](#)

[Tables](#)

[Figures](#)

◀

▶

[Back](#)

[Close](#)

[Full Screen / Esc](#)

[Printer-friendly Version](#)

[Interactive Discussion](#)



Cavity ring-down instrument for N_2O_5 , NO , NO_2 and O_3

N. L. Wagner et al.

[Title Page](#)[Abstract](#)[Introduction](#)[Conclusions](#)[References](#)[Tables](#)[Figures](#)[|◀](#)[▶|](#)[Back](#)[Close](#)[Full Screen / Esc](#)[Printer-friendly Version](#)[Interactive Discussion](#)

In this paper, we describe a single CRDS instrument based on diode lasers that measures NO_3 , N_2O_5 , NO , NO_2 , and O_3 . Unlike the previous instruments from our group, this instrument uses a diode laser near the maximum in the NO_3 absorption spectrum at 662 nm for the measurement of NO_3 and N_2O_5 (Dubé et al., 2006). This is advantageous in terms of size, weight, power consumption, and elimination of toxic dyes. The main disadvantage to this approach is its increased sensitivity to water vapor. Implications of the water vapor sensitivity for aircraft measurements are described further below. A second diode laser centered near 405 nm is used for detection of NO_2 by CRDS and of NO and O_3 by chemical conversion to NO_2 . The NO_2 channel provides not only a direct measurement of this compound, but also a method for calibrating the NO_3 and N_2O_5 measurements via the conversion of these compounds to NO_2 in excess NO as described by Fuchs et al. (2009). The NO_2 measurement is itself calibrated against a standard based on ultraviolet absorption of ozone at 254 nm as described by Washenfelder et al. (2010), providing a common analytical standard for all five species measured by this instrument.

The combination of these five trace gases provides a complete picture of the nighttime chemistry shown in Reactions (R1)–(R4). Measurements of NO_2 and O_3 provide the source for NO_3 formation. Direct measurement of NO_3 and N_2O_5 allow for understanding of their chemistry in the nighttime atmosphere. Measurement of NO characterizes one of the most important nighttime sinks for NO_3 and N_2O_5 . This paper describes the design and operation of this instrument, and its deployment on aircraft.

2 Instrument description

Cavity ring-down spectroscopy (CRDS) is commonly used for sensitive detection of trace gases and has been described in several reviews (Busch and Busch, 1999; Brown, 2003; Atkinson, 2003). CRDS is a direct absorption spectroscopy in which the optical path length is enhanced by a high finesse cavity formed by a set of two highly reflective mirrors. A laser is directed into the cavity, the optical intensity builds in

the cavity, and then the laser is quickly turned off. The subsequent exponential decay of light intensity from the cavity is monitored by measuring the light transmitted through the back mirror. When an absorber is present, the exponential decay time constant is reduced, providing an absolute measurement of optical extinction, as given in Eq. (1).

$$5 \quad \sigma[A] = \alpha = \frac{R_I}{c} \left(\frac{1}{\tau} - \frac{1}{\tau_0} \right) \quad (1)$$

Here, σ is the absorption cross-section corresponding to the absorber, center wavelength and spectrum of the laser, $[A]$ is the concentration of the absorber, α is the optical extinction coefficient (units of inverse length), c is the speed of light, τ and τ_0 are the exponential decay constants with and without the absorber in the cavity and
10 R_I is the ratio of the total length of the cavity to the length over which the absorber is present.

The instrument described here consists of two largely independent parts that share a common set of electronics, data acquisition, frame and optical mounting system. The first part is the measurement of NO_3 and N_2O_5 using a diode laser centered a
15 662 nm. The second is the measurement of NO_2 , NO , and O_3 using an additional diode laser centered 405 nm. The two parts of the instrument have separate inlets that are only connected together during automated calibrations, as described further below. A schematic of the instrument is shown in Fig. 1 with $\text{NO}_3/\text{N}_2\text{O}_5$ measurement framed in red and the $\text{NO}/\text{NO}_2/\text{O}_3$ measurement framed in blue. A photo of the instrument is
20 shown in the right panel of Fig. 1.

2.1 NO_3 and N_2O_5 measurement

Previous NO_3 and N_2O_5 instruments from our group were based on cavity ring-down spectroscopy using a pulsed dye laser and a Nd:YAG laser to pump the dye laser. Diode lasers, which are available at wavelengths near the 662 nm absorption maximum of the nitrate radical, are a suitable alternative that are smaller, lighter, lower in power consumption and do not require hazardous material. Like pulsed dye lasers,
25

Cavity ring-down instrument for N_2O_5 , NO , NO_2 and O_3

N. L. Wagner et al.

[Title Page](#)

[Abstract](#)

[Introduction](#)

[Conclusions](#)

[References](#)

[Tables](#)

[Figures](#)

◀

▶

◀

▶

[Back](#)

[Close](#)

[Full Screen / Esc](#)

[Printer-friendly Version](#)

[Interactive Discussion](#)



Cavity ring-down instrument for N_2O_5 , NO , NO_2 and O_3

N. L. Wagner et al.

[Title Page](#)[Abstract](#)[Introduction](#)[Conclusions](#)[References](#)[Tables](#)[Figures](#)[|◀](#)[▶|](#)[◀](#)[▶](#)[Back](#)[Close](#)[Full Screen / Esc](#)[Printer-friendly Version](#)[Interactive Discussion](#)

Cavity ring-down instrument for N₂O₅, NO, NO₂ and O₃

N. L. Wagner et al.

[Title Page](#)[Abstract](#)[Introduction](#)[Conclusions](#)[References](#)[Tables](#)[Figures](#)[|◀](#)[▶|](#)[◀](#)[▶](#)[Back](#)[Close](#)[Full Screen / Esc](#)[Printer-friendly Version](#)[Interactive Discussion](#)

in this on-axis alignment in order to prevent potentially damaging back reflections from entering the laser. The isolators consist of a single linear polarizer that is placed in front of the laser, and three separate quarter waveplates; one placed directly in front of each cavity. This design ensures that the polarization through the beamsplitters remains linear, so that the polarization sensitivity of the beamsplitters does not degrade the performance of the isolators.

The cavities consist of two 25 mm diameter, 1 m radius of curvature high-reflectivity dielectric mirrors. The mirrors are separated by 93 cm and mounted to an optical breadboard in a custom bellows mount that allows optical alignment and a flexible seal to the sample volume, from which the mirrors themselves are isolated. The cleanliness of the mirrors is maintained by a small purge flow, 25 sccm, of ultrapure air (zero air) over each mirror to separate the mirror surface from the sample flow. Light transmitted through the back mirror of the each cavity is collected by an optical fiber and detected on a photomultiplier tube (PMT) (Hamamatsu HC120-05M). A bandpass filter centered at 660 nm is used immediately before the PMT to reject stray light.

The ring-down traces are digitalized using 14-bit oscilloscope card (National Instruments PCI-6132) at a rate of 2.5×10^6 samples s⁻¹. A digital output of the oscilloscope card is used to modulate the laser intensity normally at 500 Hz, but this can be adjusted to increase the number of ring-down traces acquired or duration of each ring-down trace. The ring-down traces are transferred to a computer over the PCI bus and co-added in lots of 100. The number of ring-down traces in each lot can be adjusted to correspond with the laser modulation frequency and the desired measurement frequency. The co-added ring-down traces are then fit to a single exponential decay. The ring-down traces are fit using the techniques described by Everest and Atkinson (2008). Usually, the digital Fourier transform method is used; however the linear, LRS, and Levenberg-Marquardt methods are also available. When using the linear fitting method, the laser is turned off after every lot of 100 ring-down traces to measure the zero level of the PMTs. During ambient sampling, only the fit parameters are saved and ring-down traces are discarded after fitting.

The upper panel of Fig. 2 shows a co-added ring-down trace acquired while sampling laboratory air at a cell pressure of 504.6 hPa. The $1/e$ time constant for this ring-down trace is $217.98 \pm 0.05 \mu\text{s}$ where the error is the covariance of the fit parameter. The time constant is determined by the combination of Rayleigh scattering losses, mirror reflectivity, and cavity alignment. Mirror reflectivity is 99.999%, or 10 ppm transmission. The lower panel in Fig. 2 shows the fit residual as a percentage of the ring-down trace. Higher reflectivity mirrors (Advanced Thin Films, Inc.) with $R = 99.9995\%$ (5 ppm transmission) have also been used in this instrument and give a ring-down time constant in excess of 400 μs at 500 mbar pressure. All of the performance characteristics described in this paper have been achieved with the lower reflectivity mirrors, which give a larger intensity throughput and allow a higher repetition rate. Instrument performance with the higher reflectivity mirrors is not substantially different, however. For the lower reflectivity mirrors, the laser is modulated at 500 Hz, and 0.2 s is needed to acquire 100 ring-down traces; thus the overall signal acquisition rate should be 5 Hz. However, due to overhead from transferring ring-down traces to the computer memory, fitting the ring-down traces, and auxiliary measurements, the actual data acquisition rate of the measurement is currently limited to 3 Hz.

The sampling and inlet configuration for NO_3 and N_2O_5 is equivalent to that described by Fuchs et al. (2008) and is described only briefly here. Because NO_3 and N_2O_5 are reactive gases, the shortest possible residence time is needed in order to minimize wall losses for NO_3 , which has been shown previously to have a first order loss with respect to reactions on the inlet walls of approximately 0.2 s^{-1} (Dubé et al., 2006).

The inlet consists of several parts and is shown in Fig. 1. The first is a short length of 0.4 cm inner diameter Teflon tubing to bring ambient air from outside into the aircraft or instrument enclosure. Following this there are addition points for NO used to determine the instrument zero, zero air used to overflow the inlet, and $\text{NO}_3/\text{N}_2\text{O}_5$ additions for calibration. Next, a short length of 1.6 mm inner diameter tubing is used as a flow restriction to drop the pressure to approximately half of ambient. A Teflon membrane

[Title Page](#)[Abstract](#)[Introduction](#)[Conclusions](#)[References](#)[Tables](#)[Figures](#)[|◀](#)[▶|](#)[Back](#)[Close](#)[Full Screen / Esc](#)[Printer-friendly Version](#)[Interactive Discussion](#)

Cavity ring-down instrument for N₂O₅, NO, NO₂ and O₃

N. L. Wagner et al.

[Title Page](#)[Abstract](#)[Introduction](#)[Conclusions](#)[References](#)[Tables](#)[Figures](#)[|◀](#)[▶|](#)[◀](#)[▶](#)[Back](#)[Close](#)[Full Screen / Esc](#)[Printer-friendly Version](#)[Interactive Discussion](#)

Cavity ring-down instrument for N₂O₅, NO, NO₂ and O₃

N. L. Wagner et al.

[Title Page](#)[Abstract](#)[Introduction](#)[Conclusions](#)[References](#)[Tables](#)[Figures](#)[|◀](#)[▶|](#)[◀](#)[▶](#)[Back](#)[Close](#)[Full Screen / Esc](#)[Printer-friendly Version](#)[Interactive Discussion](#)

is added to the inlet flow to produce an NO concentration of $\sim 10^{12}$ molecules cm⁻³, designed to give >99.9% conversion of NO₃ to NO₂ before the flow enters the axis of the NO₃ measurement cell. The zero of the instrument is typically 5 s in duration and is measured at arbitrary intervals depending on requirements. During aircraft ascent and descent, when changes in pressure lead to rapid changes in background time constant due to Rayleigh scattering, the zero interval can be as short as once per minute. On level flight legs or for ground based measurements, a zero interval of 3–5 min is normally sufficient to track any changes in τ_0 due to cavity alignment or variable background absorbers.

10 2.2 NO, NO₂, and O₃ measurement

Measurement of NO₂ is integral to the NO₃ and N₂O₅ calibrations and measurements of inlet transmission. Measurement of NO₂ using a diode laser center at 405 nm improves its sensitivity compared to our previously described, 532 nm instrument (Osthoff et al., 2006; Fuchs et al., 2010), since the NO₂ cross-section is approximately 4× larger at 405 nm. Furthermore, the interference from ozone is essentially eliminated, since its absorption cross-section is approximately 10⁴ times smaller than that of NO₂ at 405 nm. Both NO and O₃ can be measured by the same instrument via conversion to NO₂; conversion of NO to NO₂ in excess ozone has been described previously by Fuchs et al. (2009), while conversion of O₃ to NO₂ in excess NO has been described by Washenfelder et al. (2011).

A second diode laser centered a 405 nm (Power Technology Inc., Fabry-Perot diode model IQμ series) provides the light source for the CRDS detection of NO₂. While this diode laser is not actively temperature tuned, it is held at a constant 20 °C. We have found the center wavelength to be stable over the lifetime of the laser by repeated checks against a calibrated grating spectrometer. The laser output power of 80 mW is divided into three equal parts using a 33% beamsplitter and a 50% beamsplitter. The three cavities are constructed in the same manner as the 662 nm cavities, except that a

Cavity ring-down instrument for N_2O_5 , NO , NO_2 and O_3

N. L. Wagner et al.

[Title Page](#)[Abstract](#)[Introduction](#)[Conclusions](#)[References](#)[Tables](#)[Figures](#)[|◀](#)[▶|](#)[Back](#)[Close](#)[Full Screen / Esc](#)[Printer-friendly Version](#)[Interactive Discussion](#)

bandpass filter centered at 405 nm is used in front of the photomultiplier to reject stray light. The layout is shown schematically in Fig. 1.

The data acquisition for the 405 nm channels is done in the same way as for the 662 nm channels using a second oscilloscope card to modulate the laser and acquire the ring-down down traces. The 405 nm mirrors have a reflectivity of 99.9965% (35 ppmv transmission) and give typical background time constants of 40 µs at a pressure of 840 hPa. Because the time constants on the 405 nm cavities are shorter than the 662 nm cavities, the laser is modulated at four times the frequency, or 2 kHz. Ring-down traces are acquired in lots of 400 and co-added to achieve the same overall data acquisition rate (3 Hz) as the 662 nm side of the instrument. It is not required that both the 662 nm channels and the 405 nm channels acquire the ring-down traces in lots corresponding to equal acquisition time but doing so maximizes the total number of ring-down traces collected.

The NO, NO_2 and O_3 sample cells have a separate inlet from the $\text{NO}_3/\text{N}_2\text{O}_5$ measurement, and the inlet is simpler because the 405 nm cavities are operated at ambient pressure and the measured species are less reactive. Ambient air is drawn in through a length of 0.4 cm inner diameter to a 1 µm pore size Teflon filter (Pall Corp. R2PL047) in a commercial, PFA Teflon mount (Savillex). The smaller pore-size filter ensures rejection of smaller size aerosol to which the 405 nm channels may in principle be more sensitive. Loss of NO, NO_2 and O_3 on these filters is negligible. There is no evidence for a signal due to aerosol extinction on the downstream side of these filters during sampling in ambient air. Following the filter, the flow is split into three equal parts and delivered to the sample cells. Before entering each sample cell, there is a reactor consisting of a 33 cm length of 0.95 cm inner diameter tubing. The flow rate through each channel is controlled at 2.7 LPM (volumetric) to maintain a residence time of 0.6 s (plug flow) within each reactor while sampling from variable external pressure from aircraft. On the first channel used for the NO_2 measurement, the purpose of the “reactor” is only to match the residence time of all three channels, so that NO_2 may be accurately subtracted from NO_x or O_x , as described below.

Cavity ring-down instrument for N₂O₅, NO, NO₂ and O₃

N. L. Wagner et al.

[Title Page](#)

[Abstract](#)

[Introduction](#)

[Conclusions](#)

[References](#)

[Tables](#)

[Figures](#)

◀

▶

[Back](#)

[Close](#)

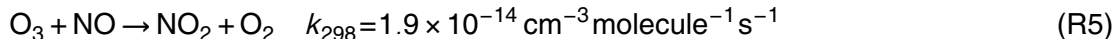
[Full Screen / Esc](#)

[Printer-friendly Version](#)

[Interactive Discussion](#)



The second channel measures total NO_x via conversion of NO to NO₂ in excess O₃. A 12 sccm flow of ~3 parts per thousand (ppthv) ozone is added at the beginning of the reactor via a three way valve that allows switching of this ozone addition to a vent line. The ozone is generated by passing a flow of pure oxygen over a mercury-argon lamp (UVP 90-0004-01). The resulting ozone concentration in the sample cell is approximately 4×10^{14} (~16 ppmv at 1 atm and 298 K) and is measured periodically from the change in optical extinction at 405 nm ($\sim 6 \times 10^{-9} \text{ cm}^{-1}$) upon switching the ozone flow into and out of the sample cell. This measurement is checked less frequently using a commercial ozone monitoring instrument. The background extinction due to this added ozone changes the ring-down time constant by approximately 0.25 μs from its nominal value of 40 μs at 1 atm. The presence of this large excess ozone converts NO quantitatively to NO₂ via Reaction (R5).



Conversion of NO to NO₂ under these reactor conditions is greater than 99%. A small correction of 1–2% is required to account for the further oxidation of NO₂ to higher oxides of nitrogen, NO₃ and N₂O₅, via Reactions (R1) and (R2) (Fuchs et al., 2009). The measured NO_x concentration is also corrected for the small dilution (~0.5%) due to the addition of the O₃/O₂ flow.

The third channel measures total odd oxygen, O_x = NO₂ + O₃, via the analogous conversion of O₃ to NO₂ in excess NO. A small flow of NO from a standard mixture of NO in N₂ (Scott-Marin) is added at the beginning of the reactor to produce an excess concentration of NO identical to the excess O₃ concentration in the NO_x channel (i.e., 4×10^{14} molecules cm⁻³). The excess NO quantitatively (greater than 99%) converts O₃ in the ambient sample flow to NO₂ via Reaction (R5). There is no need for an additional correction for further oxidation of NO₂ on this channel since Reactions (R1)–(R2), to the small extent that they might occur without large, excess O₃, are effectively reversed by reaction of NO₃ with the excess NO (Reaction R4). The excess NO added to this channel does contain an unavoidable contamination of NO₂, which can produce

a large background signal. An FeSO_4 converter on the outlet of the standard cylinder reduces this NO_2 contamination considerably to a background level of 0.5–2 ppbv within the sample cell (Washenfelder et al., 2011).

Maintaining a constant number density of excess O_3 or NO on either the NO_x or O_x channel is a potential challenge for sampling from an aircraft platform since the ambient pressure is variable with aircraft altitude. Flows on all three 405 nm channels are controlled at constant volumetric rates by varying the standard flow rate with ambient pressure to maintain constant residence time in each reactor. Addition of a constant, standard flow of excess reagent with a well-defined mixing ratio to the variable, volumetric flow produces a constant number density in each reactor as the aircraft ascends and descends. Thus, the conversion efficiencies outlined above do not vary with aircraft altitude.

The current scheme for acquiring a zero time constant for the 405 nm channels is identical to that used previously with our 532 nm CRDS NO_2 instrument, namely to slightly overflow the inlet with zero air. The overflow is added through a concentric piece of Teflon tubing with an inner diameter slightly larger than the outer diameter of the inlet tubing and which extends slightly (2–4 cm) beyond the inlet tubing. Addition through this concentric inlet minimizes the pressure difference between the zero and signal measurement, which can be significant (1 hPa or greater) if the zero air overflow is added through a simple tee fitting. Such pressure differences between the zero and sample measurement change the Rayleigh scattering background, which must be corrected for after the measurement. An additional correction is needed to account for the difference in humidity between ambient air and the dry zero air used to overflow the inlet. The difference in the Rayleigh scattering cross-section of water vapor and air was measured at 405 nm by Fuchs et al. (2009) to be $5 \times 10^{-27} \text{ cm}^2$, leading to a maximum correction equivalent to 0.15 ppbv NO_2 at 80% RH (22 °C). Actual water vapor corrections are typically smaller, however. Zero measurements occurred every 3 min during ambient sampling and lasted 15 s to allow for the zero air to completely fill the sample cell.

Title Page	
Abstract	Introduction
Conclusions	References
Tables	Figures
◀	▶
◀	▶
Back	Close
Full Screen / Esc	
Printer-friendly Version	
Interactive Discussion	



[Title Page](#)[Abstract](#)[Introduction](#)[Conclusions](#)[References](#)[Tables](#)[Figures](#)[|◀](#)[▶|](#)[Back](#)[Close](#)[Full Screen / Esc](#)[Printer-friendly Version](#)[Interactive Discussion](#)

The optical extinction due to excess O_3 on the NO_x channel, and the NO_2 impurity in the added NO on the O_x channel, are not affected by the addition of zero air to the inlet. Thus, no correction is required for these small, background optical extinctions.

3 Calibrations

- 5 Although cavity ring down spectroscopy is, in principle, an absolute method, calibrations are required if either the inlet transmission efficiency for a particular trace gas is not unity, or if the absorption cross-section can vary as a function of sampling conditions (i.e., temperature, pressure). The former is the case for NO_3 and N_2O_5 , which are reactive trace gases whose transmission through the inlet system may vary. The
- 10 latter is potentially the case for NO_2 (and by extension, NO and O_3 in this instrument) since its absorption cross-section varies with pressure and temperature. We have recently developed calibration standards for NO_3 and N_2O_5 based on their conversion to NO_2 (Fuchs et al., 2008) and for NO_2 based on conversion of a standard additions of O_3 , as described above (Washenfelder et al., 2011). The following sections outline these calibration schemes and their implementation in the current version of this aircraft instrument.

3.1 NO_2 calibration

- 20 The 405 nm laser diodes provided by the manufacturer vary in center wavelength; hence, the effective cross-section for each laser must be calibrated by standard NO_2 additions. Standard concentrations of O_3 are generated and measured using a commercial ozone monitor, then quantitatively converted to NO_2 , which is measured on the CRDS instrument, as described above. The calibrator contains its own NO cylinder and flow controllers for conversion of O_3 to NO_2 such that it delivers standard additions of NO_2 independent from the CRDS instrument itself. The calibrator is also field portable and can be used for routine calibration on a daily basis. Typical calibration

Cavity ring-down instrument for N_2O_5 , NO , NO_2 and O_3

N. L. Wagner et al.

[Title Page](#)[Abstract](#)[Introduction](#)[Conclusions](#)[References](#)[Tables](#)[Figures](#)[|◀](#)[▶|](#)[◀](#)[▶](#)[Back](#)[Close](#)[Full Screen / Esc](#)[Printer-friendly Version](#)[Interactive Discussion](#)

curves use a series of NO_2 mixing ratios between 0–200 ppbv, with the effective NO_2 cross-section determined as the slope of a plot of measured optical extinction against NO_2 concentration.

The cell pressure in the 405 nm channels varies significantly with altitude, typically between 500 and 900 hPa over the altitude range of the NOAA WP-3 aircraft and is typically 80–100 hPa below ambient pressure. Therefore, any pressure dependence in the absorption cross-section for NO_2 will directly affect the measurement from aircraft. Literature spectra for NO_2 do indeed show a pressure dependence, e.g., Vandaele et al. (1998), but only for spectral features too fine to be resolved by the laser system in the CRDS instrument. Nevertheless, effective NO_2 absorption cross-section under the bandwidth of the diode laser used here shows a distinct pressure dependence. Figure 3 shows the NO_2 cross-section calibration as a function of pressure. The NO_2 cross-section decreases by approximately 6% between 1000 and 500 hPa. The calibration curve in Fig. 3 is the result of multiple determinations in the field on different days, which were reproducible at any given pressure to within $\pm 2\%$. For the purpose of calculating the NO_2 concentration, the cross-section is parameterized by a 3rd order polynomial. The NO_2 absorption cross-section is likely to be temperature-dependent as well; however, the current version of this instrument has been operated within a temperature range from 25–32 °C, over which the change in cross-section is not measurable. Temperature control on the 405 nm channels may be incorporated in the future if sampling in a variable temperature environment is required.

3.2 NO_3 cross-section and water vapor sensitivity

The cross-section for NO_3 is determined using the absorption spectrum measured by Yokelson et al. (1994) shown in Fig. 4 and temperature-dependence determined by Osthoff et al. (2007). Although the absorption spectrum peaks at $2.17 \times 10^{-17} \text{ cm}^2$ for 298 K the effective cross-section in this instrument is a convolution of the measured cross-section and the laser spectrum and is therefore smaller than the peak absorption. Using a typical laser spectrum shown Fig. 4, the effective cross-section was

Cavity ring-down instrument for N₂O₅, NO, NO₂ and O₃

N. L. Wagner et al.

[Title Page](#)[Abstract](#)[Introduction](#)[Conclusions](#)[References](#)[Tables](#)[Figures](#)[|◀](#)[▶|](#)[Back](#)[Close](#)[Full Screen / Esc](#)[Printer-friendly Version](#)[Interactive Discussion](#)

$2.03 \times 10^{-17} \text{ cm}^2$, a reduction of 7%. One drawback of 662 nm diode laser used in this instrument is that the intensity in different modes, and thus is spectral output, is not stable on the time scale of hours. Based on several measured laser spectra, this instability leads to a variation of 1.5% in the effective NO₃ cross-section. The uncertainty in this cross-section is given by Fuchs et al. (2008) as $\pm 4\%$; in this instrument, this increases to $\pm 6\%$ due to laser spectral variability. The laser spectrum is currently measured infrequently (e.g., once per flight) using a small grating spectrometer (Ocean Optics, USB4000) but will be incorporated into routine data acquisition in the future. The NO₃ cross-section is temperature dependent, as described previously, such that the effective cross-section for the heated channel is $1.68 \times 10^{-17} \text{ cm}^2 \text{ molecule}^{-1}$ at 348 K.

Water vapor has an absorption in the 662 nm region of the spectrum. The potential for water vapor interference with NO₃ measurements is well known from broadband optical measurements of NO₃, e.g., Langridge et al. (2008), Solomon et al. (1989). The water vapor spectrum at 20 °C from the HITRAN database (Rothman et al., 2011) is shown in red on Fig. 4 along with the nitrate radical absorption spectrum (blue) and typical diode laser spectrum (gray). Our previous, pulsed dye laser instrument had a narrow bandwidth which effectively resolved this water vapor spectrum, and could be tuned off resonance with the discrete water vapor lines while still being tuned effectively to the maximum in the NO₃ absorption spectrum. The output of the diode laser, by contrast, unavoidably overlaps multiple water vapor lines, making the instrument much more sensitive to this interference. Furthermore, because the water vapor absorption spectrum consists of several peaks under the laser bandwidth, the variation in absorption cross-section can lead to non-exponential ring down traces.

The measured sensitivity to water vapor is shown in Fig. 4 (lower panel). The extinction is not linear with respect to water concentration because the ring-down transients become slightly non-exponential at higher optical extinctions because of the mismatch between the discrete, water vapor lines and the broadband laser source (Zalicki and Zare, 1995). However, the data can be corrected by using the fitted polynomial as an

effective concentration-dependent cross-section as shown in Eq. (2).

$$\tau_{\text{corrected}} = \left(\frac{1}{\tau} + \frac{f([\text{H}_2\text{O}])c}{R_I} \right)^{-1} \quad (2)$$

$\tau_{\text{corrected}}$ is the time exponential decay time constant that would be measured in the absence of water vapor. τ is the measured exponential decay constant. $f([\text{H}_2\text{O}])$ is the fitted polynomial sensitivity and requires an independent measurement of the water vapor mixing ratio. The linear term in the polynomial fit corresponds to the water vapor cross-section when averaged over the laser spectrum and agrees well with the value calculated using the water vapor cross-section obtained from the HITRAN database, $2.05 \times 10^{-26} \text{ cm}^2$. This linear absorption is insensitive to the presence of added NO, and will therefore only interfere with the measurement of NO_3 and N_2O_5 if the water vapor mixing ratio changes rapidly on the time scale of the instrument zero frequency. Such variations can, in principle, be corrected by the reference channel (see above), though in practice the active correction described here proved as useful as a reference channel. For ground based measurements, simple interpolation between zeros would normally be sufficient. However, for aircraft sampling, which may rapidly traverse regions of higher or lower absolute humidity (e.g., on vertical profiles), the interferences must be actively corrected via Eq. (2). A worst-case change in relative humidity from 0 to 100%, or $3.5 \times 10^{17} \text{ cm}^{-3}$ (2.9% mixing ratio at 20 °C and 505 hPa in the sample cells), would result in an additional extinction of $7 \times 10^{-9} \text{ cm}^{-1}$, or the equivalent of 30 pptv of $\text{NO}_3/\text{N}_2\text{O}_5$. In practice, we have never observed variations in background extinction that are this extreme; however active correction remains a necessity.

When the water vapor concentration is approximately constant between the zero and the signal measurement, there is an additional, small error due to fitting the slightly non-exponential ring-down transients in the presence of water vapor as though they were single exponentials to retrieve concentrations of NO_3 or N_2O_5 . This effect produces a measurement error of less than 0.2% for either compound.

Cavity ring-down instrument for N_2O_5 , NO , NO_2 and O_3

N. L. Wagner et al.

[Title Page](#)

[Abstract](#)

[Introduction](#)

[Conclusions](#)

[References](#)

[Tables](#)

[Figures](#)

◀

▶

◀

▶

[Back](#)

[Close](#)

[Full Screen / Esc](#)

[Printer-friendly Version](#)

[Interactive Discussion](#)



3.3 NO_3 and N_2O_5 inlet transmission

Wall loss of NO_3 on the Teflon surfaces of the inlet and measurement cells is the most significant source of uncertainty for CRDS measurement of NO_3 and N_2O_5 (Dubé et al., 2006). Characterization of the NO_3 and N_2O_5 transmission efficiency has been described by Fuchs et al. (2008). The following provides a short description of the method and the changes that are specific to the current instrument design. The calibration scheme for NO_3 is based on its chemical conversion to NO_2 with excess NO by Reaction (R4), the same as used for zeroing the 662 nm channels. The resulting NO_2 has negligible inlet loss and can be measured by CRDS at 405 nm to provide a standard for the 662 nm NO_3 measurement. N_2O_5 can be measured similarly by chemical and thermal conversion to NO_2 .

As described above, for ambient sampling, the inlet for the NO_2 , NO_x and O_x channels is separate from the NO_3 and N_2O_5 inlet. The calibration scheme uses only the NO_2 channel, but it must be connected to the inlet for NO_3 and N_2O_5 . This connection is made via the three-way valve shown in Fig. 1, which switches the instrument between sampling and calibration mode. Unlike the previously described calibration scheme, in which the NO_3 and NO_2 measurements were in series, they are in parallel in this configuration, such that measurements of NO_3 or N_2O_5 occur simultaneously with that of NO_2 . The connection to the NO_2 sample cell has a heater to convert N_2O_5 to NO_3 followed by a short section of nylon tubing which acts as an NO_3 scrubber, as described in Fuchs et al. (2008). In this configuration, the scrubber serves to remove NO_3 from the flow exiting the heater when the NO addition is off, so that the calibration channel measures only the NO_2 arising from thermal dissociation of N_2O_5 and not any optical extinction from NO_3 . It also prevents recombination of NO_3 with NO_2 in the calibration channel. During addition of NO, all NO_3 produced in the heater between the inlet and the calibration channel is converted to $2 \times \text{NO}_2$, which is not affected by the scrubber.

Title Page	
Abstract	Introduction
Conclusions	References
Tables	Figures
◀	▶
◀	▶
Back	Close
Full Screen / Esc	
Printer-friendly Version	
Interactive Discussion	

Cavity ring-down instrument for N₂O₅, NO, NO₂ and O₃

N. L. Wagner et al.

[Title Page](#)

[Abstract](#)

[Introduction](#)

[Conclusions](#)

[References](#)

[Tables](#)

[Figures](#)

◀

▶

[Back](#)

[Close](#)

[Full Screen / Esc](#)

[Printer-friendly Version](#)

[Interactive Discussion](#)



Calibration samples of N₂O₅ or NO₃ are generated by passing a small flow of zero air over a sample of solid N₂O₅ stored in a trap at -78 °C (dry ice). The source produces N₂O₅ with less than 2% NO₃ or, if switched through a heater mounted in the calibration box, greater than 90% NO₃. The NO₃ (N₂O₅) concentration, reduced by inlet loss, is measured by 662 nm optical extinction. Titration of this NO₃ (N₂O₅) by NO produces NO₂, which is measured quantitatively by optical extinction at 405 nm.

There are two other sources of NO₂ that contribute to its background during calibrations. The first is the NO₂ that comes directly off the solid N₂O₅ trap, which can be measured while adding only NO₃ or N₂O₅ to the inlet. Second, the standard NO cylinder has an unavoidable NO₂ contamination (typically 0.3% of the NO mixing ratio), which can be measured by adding only NO to the inlet without NO₃. Equation (3) then gives the expression for the transmission efficiency as the ratio between measured NO₃ in the 662 nm channel and 1/2 the NO₂ generated from the conversion in Reaction (R4).

$$T_e = \frac{2 [NO_3]}{[NO_2]_{Trap+NO} - [NO_2]_{Trap} - [NO_2]_{NO}} \quad (3)$$

Here, [NO₂]_{Trap+NO} is the NO₂ concentration when both the NO₃ and NO are added to the inlet, and [NO₂]_{Trap} and [NO₂]_{NO} are the NO₂ concentrations when the NO₃ and NO are added to the inlet separately.

Three separate transmission efficiencies are required: (1) the transmission of N₂O₅ through the heated inlet, $T_e(N_2O_5)$, which is the combination of the transmission efficiency for N₂O₅ itself, the conversion efficiency to NO₃, and the transmission of NO₃ through the heated inlet; (2) the transmission of NO₃ through the ambient channel, $T_e^{ambient}(NO_3)$; and (3) the transmission of NO₃ through the heated channel, $T_e^{heated}(NO_3)$ (Dubé et al., 2006; Fuchs et al., 2008). For the NO₃ channel only the inlet transmission of NO₃ is needed to determine the ambient NO₃ concentration, Eq. (4). However, because N₂O₅ is converted to NO₃ in the inlet and consequently lost to the walls, the inlet transmission of both NO₃ and N₂O₅ is needed to calculate the ambient

N_2O_5 concentration, Eq. (5).

$$[\text{NO}_3]_{\text{amb}} = \frac{[\text{NO}_3]_{\text{cell}}}{T_e^{\text{ambient}}(\text{NO}_3)} \quad (4)$$

$$[\text{N}_2\text{O}_5]_{\text{amb}} = \frac{([\text{NO}_3] + [\text{N}_2\text{O}_5])_{\text{cell}} - T_e^{\text{heated}}(\text{NO}_3)[\text{NO}_3]_{\text{amb}}}{T_e(\text{N}_2\text{O}_5)} \quad (5)$$

$[\text{NO}_3]_{\text{amb}}$ and $[\text{N}_2\text{O}_5]_{\text{amb}}$ are the ambient concentration of NO_3 and N_2O_5 . $[\text{NO}_3]_{\text{cell}}$ and $([\text{NO}_3] + [\text{N}_2\text{O}_5])_{\text{cell}}$ are the concentrations measured in the sample cells.

Figure 5 illustrates the scheme for an example calibration. Panel A shows the N_2O_5 transmission measurement, while panel B shows the NO_3 transmission measurements in both the ambient and heated measurement cells, which is done simultaneously by addition of NO_3 to both channels.

10 4 Detection limits and sample data

Figure 6 shows a representative measurement of the NO_3 and N_2O_5 instrument baseline precision in our laboratory while sampling zero air. The Allan variance plot gives a detection limit under ~ 1 pptv (2σ) in 1 s for both species. For NO_3 , this sensitivity is comparable to, but slightly worse than that reported by Dubé et al. (2006) (e.g., 0.5 pptv, 1 s, 2σ) using the Nd:YAG/dye laser instrument. For N_2O_5 , the sensitivity is slightly improved over the pulsed laser version (e.g., 2 pptv, 1 s, 2σ), although the latter improvement derives more from reduction in the optical noise associated with the fast flow in the heated channel than with any change in the optical system itself. The detection limits for the NO , NO_2 and O_3 measurements have been reported in a separate publications (Washenfelder et al., 2011; Fuchs et al., 2009) and are 170 pptv, 46 pptv and 56 pptv (1 s, 2σ), respectively. Our previously reported, ground based NO_x instrument (Fuchs et al., 2009) exhibits a better precision of 22 pptv (2σ , 1 s). The aircraft measurements of NO , NO_2 and O_3 also suffer from an optical instability in flight that leads

Title Page	Abstract	Introduction
Conclusions	References	
Tables	Figures	
◀	▶	
◀	▶	
Back	Close	
Full Screen / Esc		
	Printer-friendly Version	
	Interactive Discussion	



**Cavity ring-down instrument for N_2O_5 ,
NO, NO_2 and O_3**

N. L. Wagner et al.

[Title Page](#)[Abstract](#)[Introduction](#)[Conclusions](#)[References](#)[Tables](#)[Figures](#)[|◀](#)[▶|](#)[◀](#)[▶](#)[Back](#)[Close](#)[Full Screen / Esc](#)[Printer-friendly Version](#)[Interactive Discussion](#)

Cavity ring-down instrument for N₂O₅, NO, NO₂ and O₃

N. L. Wagner et al.

[Title Page](#)

[Abstract](#)

[Introduction](#)

[Conclusions](#)

[References](#)

[Tables](#)

[Figures](#)

◀

▶

◀

▶

[Back](#)

[Close](#)

[Full Screen / Esc](#)

[Printer-friendly Version](#)

[Interactive Discussion](#)



NO and modifications of inlet and sample flow path for improved time response of all channels (Pollack et al., 2011). The right three panels of Fig. 8 show the scatter plots comparing NO, NO₂, and O₃ measurements from the 405 nm CRDS instrument with those from the CL instrument at 1 s time resolution. The instruments agree to within 3% for NO, 5% for NO₂, and 1% for O₃ measurements. Correlation among all measurements was excellent, with R^2 values ≥ 0.99 . Much of the scatter in the correlation plots is the result of synchronization between the instruments when transecting NO_x plumes with sharp edges. Although CRDS is lower in precision than the CL instrument and is subject to some baseline instability as described above, the comparisons in Fig. 8 demonstrate that it is accurate, at least at larger NO_x and O₃ values.

One common diagnostic used to understand the nighttime reactivity of NO₃ and N₂O₅ is their steady state atmospheric lifetime (Platt et al., 1984). The steady state lifetime of a species can be determined from its rate of production and its concentration, defined in Eqs. (6) and (7) for NO₃ and N₂O₅ (Brown et al., 2003).

$$\tau_{\text{SS}}(\text{NO}_3) = \frac{[\text{NO}_3]}{k_1 [\text{O}_3][\text{NO}_2]} \approx \left(k_{\text{NO}_3} + k_{\text{N}_2\text{O}_5} K_{\text{eq}}[\text{NO}_2] \right)^{-1} \quad (6)$$

$$\tau_{\text{SS}}(\text{N}_2\text{O}_5) = \frac{[\text{N}_2\text{O}_5]}{k_1 [\text{O}_3][\text{NO}_2]} \approx \left(k_{\text{N}_2\text{O}_5} + \frac{k_{\text{NO}_3}}{K_{\text{eq}}[\text{NO}_2]} \right)^{-1} \quad (7)$$

Here $\tau_{\text{SS}}(\text{NO}_3)$ and $\tau_{\text{SS}}(\text{N}_2\text{O}_5)$ are the steady state lifetimes and k_1 is the rate constant for Reaction (R1). When the steady state approximation is valid the lifetimes can be used to determine the pseudo first-order loss rate of NO₃ and N₂O₅, k_{NO_3} and $k_{\text{N}_2\text{O}_5}$. K_{eq} is the equilibrium constant for Reaction (R2). In past field campaigns, this analysis would require data from at least two separate instruments. Figure 8 demonstrates the advantage of the combined measurements of nighttime nitrogen oxides (NO₂, NO₃ and N₂O₅) and O₃ into a single instrument. Figure 9 shows the steady state lifetimes for the flight of 30 May. The lifetimes of NO₃ range from 0 to 1.5 h and lifetimes up to 3 h are observed for N₂O₅. Thus, the combination of NO₂, O₃ with NO₃ and N₂O₅, all

tied to a single analytical standard, provides a complete and accurate representation of nighttime nitrogen oxide chemistry.

AMTD

4, 1555–1591, 2011

5 Conclusions

The article has described an aircraft instrument for atmospheric measurements of NO_3 , N_2O_5 , NO, NO_2 , and O_3 by cavity ring-down spectroscopy. NO_3 and NO_2 are measured directly using a diode lasers with center wavelengths of 662 nm and 405 nm. N_2O_5 is thermally converted to NO_3 for measurement and NO and O_3 are chemically converted to NO_2 and measured. Each channel is regularly calibrated in the field by a scheme linking the cross-sections of each channel to the O_3 cross-section at 254 nm. The inlet transmission of NO_3 and N_2O_5 is also measured regularly in the field. The performance of the instrument was demonstrated during its first deployment on the NOAA P-3 in California during a 2010 field intensive.

Acknowledgements. This work was funded in part by NOAA's Atmospheric Chemistry and Climate Program.

15 References

- Atkinson, D. B.: Solving chemical problems of environmental importance using cavity ring-down spectroscopy, *Analyst*, 128, 117–125, doi:10.1039/b206699h, 2003.
- Atkinson, R.: Kinetics and mechanisms of the gas-phase reactions of the NO_3 radical with organic-compounds, *J. Phys. Chem. Ref. Data*, 20(3), 459–507, doi:10.1063/1.555887, 1991.
- Ayers, J. D., Apodaca, L., Simpson, W. R., and Baer, D. S.: Off-axis cavity ring-down spectroscopy: Application to atmospheric nitrate radical detection, *Appl. Optics*, 44, 7239–7242, doi:10.1364/AO.44.007239, 2005.
- Brown, S. S., Stark, H., Ciciora, S. J., McLaughlin, R. J., and Ravishankara, A. R.: Simultaneous in situ detection of atmospheric NO_3 and N_2O_5 via cavity ring-down spectroscopy, *Rev. Sci. Instrum.*, 73, 3291–3301, doi:10.1063/1.1499214, 2002.

Discussion Paper | Discussion Paper

Discussion Paper | Discussion Paper

Discussion Paper | Discussion Paper

Cavity ring-down instrument for N_2O_5 , NO, NO_2 and O_3

N. L. Wagner et al.

Title Page

Abstract

Introduction

Conclusions

References

Tables

Figures

◀

▶

◀

▶

Back

Close

Full Screen / Esc

Printer-friendly Version

Interactive Discussion



Brown, S. S.: Absorption spectroscopy in high-finesse cavities for atmospheric studies, *Chem. Rev.*, 103, 5219–5238, doi:10.1021/cr020645c, 2003.

Brown, S. S., Stark, H., and Ravishankara, A. R.: Applicability of the steady state approximation to the interpretation of atmospheric observations of NO_3 and N_2O_5 , *J. Geophys. Res.-Atmos.*, 108(D17), 4539, doi:10.1029/2003JD003407, 2003.

Brown, S. S., Dubé, W. P., Osthoff, H. D., Stutz, J., Ryerson, T. B., Wollny, A. G., Brock, C. A., Warneke, C., de Gouw, J. A., Atlas, E., Neuman, J. A., Holloway, J. S., Lerner, B. M., Williams, E. J., Kuster, W. C., Goldan, P. D., Angevine, W. M., Trainer, M., Fehsenfeld, F. C., and Ravishankara, A. R.: Vertical profiles in NO_3 and N_2O_5 measured from an aircraft: Results from the NOAA P-3 and surface platforms during NEAQS 2004, *J. Geophys. Res.*, 112, D22304, doi:10.1029/2007JD008883, 2007a.

Brown, S. S., Dubé, W. P., Osthoff, H. D., Wolfe, D. E., Angevine, W. M., and Ravishankara, A. R.: High resolution vertical distributions of NO_3 and N_2O_5 through the nocturnal boundary layer, *Atmos. Chem. Phys.*, 7, 139–149, doi:10.5194/acp-7-139-2007, 2007b.

Busch, K. W. and Busch, M. A.: Cavity-ringdown spectroscopy, American Chemical Society, Washington, DC, 1999.

Dubé, W. P., Brown, S. S., Osthoff, H. D., Nunley, M. R., Ciciora, S. J., Paris, M. W., McLaughlin, R. J., and Ravishankara, A. R.: Aircraft instrument for simultaneous, in situ measurement of NO_3 and N_2O_5 via pulsed cavity ring-down spectroscopy, *Rev. Sci. Instrum.*, 77(3), 034101–034101-11, doi:10.1063/1.2176058, 2006.

Everest, M. A. and Atkinson, D. B.: Discrete sums for the rapid determination of exponential decay constants, *Rev. Sci. Instrum.*, 79, 023108, doi:10.1063/1.2839918, 2008.

Finlayson-Pitts, B. J., Ezell, M. J., and Pitts, J. N.: Formation of chemically active chlorine compounds by reactions of atmospheric NaCl particles with gaseous N_2O_5 and ClONO_2 , *Nature*, 337, 241–244, doi:10.1038/337241a0, 1989.

Fuchs, H., Dubé, W. P., Ciciora, S. J., and Brown, S. S.: Determination of inlet transmission and conversion efficiencies for in situ measurements of the nocturnal nitrogen oxides, NO_3 , N_2O_5 and NO_2 , via pulsed cavity ring-down spectroscopy, *Anal. Chem.*, 80, 6010–6017, doi:10.1021/ac8007253, 2008.

Fuchs, H., Dubé, W. P., Lerner, B. M., Wagner, N. L., Williams, E. J., and Brown, S. S.: A sensitive and versatile detector for atmospheric NO_2 and NO_x based on blue diode laser cavity ring-down spectroscopy, *Environ. Sci. Technol.*, 43, 7831–7836, doi:10.1021/es902067h, 2009.

[Title Page](#)[Abstract](#)[Introduction](#)[Conclusions](#)[References](#)[Tables](#)[Figures](#)[|◀](#)[▶|](#)[◀](#)[▶](#)[Back](#)[Close](#)[Full Screen / Esc](#)[Printer-friendly Version](#)[Interactive Discussion](#)

Fuchs, H., Ball, S. M., Bohn, B., Brauers, T., Cohen, R. C., Dorn, H.-P., Dubé, W. P., Fry, J. L., Häseler, R., Heitmann, U., Jones, R. L., Kleffmann, J., Mentel, T. F., Msgen, P., Rohrer, F., Rollins, A. W., Ruth, A. A., Kiendler-Scharr, A., Schlosser, E., Shillings, A. J. L., Tillmann, R., Varma, R. M., Venables, D. S., Villena Tapia, G., Wahner, A., Wegener, R., Wooldridge, P. J., and Brown, S. S.: Intercomparison of measurements of NO₂ concentrations in the atmosphere simulation chamber SAPHIR during the NO3Comp campaign, *Atmos. Meas. Tech.*, 3, 21–37, doi:10.5194/amt-3-21-2010, 2010.

Jones, C. L. and Seinfeld, J. H.: The oxidation of NO₂ to nitrate – day and night, *Atmos. Environ.*, 17(11), 2370–2373, doi:10.1016/0004-6981(83)90239-1, 1983.

King, M. D., Dick, E. M., and Simpson, W. R.: A new method for the atmospheric detection of the nitrate radical (NO₃), *Atmos. Environ.*, 34(5), 685–688, doi:10.1016/S1352-2310(99)00418-5, 2000.

Langridge, J. M., Ball, S. M., Shillings, A. J., and Jones, R. L.: A broadband absorption spectrometer using light emitting diodes for ultrasensitive, in situ trace gas detection, *Rev. Sci. Instrum.*, 79, 123110, doi:10.1063/1.3046282, 2008.

Osthoff, H. D., Brown, S. S., Ryerson, T. B., Fortin, T. J., Lerner, B. M., Williams, E. J., Pettersson, A., Baynard, T., Dube, W. P., Ciciora, S. J., and Ravishankara, A. R.: Measurement of atmospheric NO₂ by pulsed cavity ring-down spectroscopy, *J. Geophys. Res.*, 111, D12305, doi:10.1029/2005JD006942, 2006.

Osthoff, H. D., Pilling, M. J., Ravishankara, A. R., and Brown, S. S.: Temperature dependence of the NO₃ absorption cross section above 298 K and determination of the equilibrium constant for NO₃+NO₂-N₂O₅ at atmospherically relevant conditions, *Phys. Chem. Chem. Phys.*, 9, 5785–5793, doi:10.1039/b709193a, 2007.

Plane, J. M. C. and Nien, C. F.: Differential optical-absorption spectrometer for measuring atmospheric trace gases, *Rev. Sci. Instrum.*, 63, 1867–1876, doi:10.1063/1.1143296, 1992.

Platt, U., Perner, D., Winer, A. M., Harris, G. W., and Pitts, J. N.: Detection of NO₃ in the polluted troposphere by differential optical-absorption, *Geophys. Res. Lett.*, 7(1), 89–92, 1980.

Platt, U. F., Winer, A. M., Bierman, H. W., Atkinson, R., and Pitts Jr., J. N.: Measurement of nitrate radical concentrations in continental air, *Environ. Sci. Technol.*, 18, 365–369, doi:10.1021/es00123a015, 1984.

Pollack, I. B., Lerner, B. M., and Ryerson, T. B.: Evaluation of ultraviolet light-emitting diodes for detection of atmospheric NO₂ by photolysis – chemiluminescence, *J. Atmos. Chem.*, in press, doi:10.1007/s10874-011-9184-3, 2011.

Title Page	Abstract	Introduction
Conclusions	References	
Tables	Figures	
◀	▶	
◀	▶	
Back	Close	
Full Screen / Esc		
Printer-friendly Version		
Interactive Discussion		



Rothman, L. S., Gordon, I. E., Barbe, A., Benner, D. C., Bernath, P. E., Birk, M., Boudon, V., Brown, L. R., Campargue, A., Champion, J. P., Chance, K., Coudert, L. H., Dana, V., Devi, V. M., Fally, S., Flaud, J. M., Gamache, R. R., Goldman, A., Jacquemart, D., Kleiner, I., Lacome, N., Lafferty, W. J., Mandin, J. Y., Massie, S. T., Mikhailenko, S. N., Miller, C. E., Moazzen-Ahmadi, N., Naumenko, O. V., Nikitin, A. V., Orphal, J., Perevalov, V. I., Perrin, A., Predoi-Cross, A., Rinsland, C. P., Rotger, M., Simeckova, M., Smith, M. A. H., Sung, K., Tashkun, S. A., Tennyson, J., Toth, R. A., Vandaele, A. C., and Vander Auwera, J.: The HITRAN 2008 molecular spectroscopic database, *J. Quant. Spectrosc. Ra.*, 110, 533–572, doi:10.1016/j.jqsrt.2009.02.013, 2011.

Ryerson, T. B., Huey, L. G., Knapp, K., Neuman, J. A., Parrish, D. D., Sueper, D. T., and Fehsenfeld, F. C.: Design and initial characterization of an inlet for gas-phase NO_y measurements from aircraft, *J. Geophys. Res.-Atmos.*, 104(D5), 5483–5492, doi:10.1029/1998JD100087, 1999.

Ryerson, T. B., Williams, E. J., and Fehsenfeld, F. C.: An efficient photolysis system for fast-response NO₂ measurements, *J. Geophys. Res.-Atmos.*, 105(D21), 26447–26461, doi:10.1029/2000JD900389, 2000.

Ryerson, T. B., Trainer, M., Angevine, W. M., Brock, C. A., Dissly, R. W., Fehsenfeld, F. C., Frost, G. J., Goldan, P. D., Holloway, J. S., Hubler, G., Jakoubek, R. O., Kuster, W. C., Neuman, J. A., Nicks, D. K., Jr., Parrish, D. D., Roberts, J. M., Sueper, D. T., Atlas, E. L., Donnelly, S. G., Flocke, F., Fried, A., Potter, W. T., Schauffler, S., Stroud, V., Weinheimer, A. J., Wert, B. P., Wiedinmyer, C., Alvarez, R. J., Banta, R. M., Darby, L. S., and Senff, C. J.: Effect of petrochemical industrial emissions of reactive alkenes and NO_x on tropospheric ozone formation in Houston, Texas, *J. Geophys. Res.*, 108, ACH8-1-24, doi:10.1029/2002jd003070, 2003.

Schuster, G., Labazan, I., and Crowley, J. N.: A cavity ring down/cavity enhanced absorption device for measurement of ambient NO₃ and N₂O₅, *Atmos. Meas. Tech.*, 2, 1–13, doi:10.5194/amt-2-1-2009, 2009.

Solomon, S., Miller, H. L., Smith, J. P., Sanders, R. W., Mount, G. H., Schmeltekopf, A. L., and Noxon, J. F.: Atmospheric NO₃, 1. Measurement technique and the annual cycle, 40° N, *J. Geophys. Res.*, 94, 11041–11048, 1989.

Thornton, J. A., Kercher, J. P., Riedel, T. P., Wagner, N. L., Cozic, J., Holloway, J. S., Dube, W. P., Wolfe, G. M., Quinn, P. K., Middlebrook, A. M., Alexander, B., and Brown, S. S.: A large atomic chlorine source inferred from mid-continental reactive nitrogen chemistry, *Nature*,

[Title Page](#)[Abstract](#)[Introduction](#)[Conclusions](#)[References](#)[Tables](#)[Figures](#)[◀](#)[▶](#)[◀](#)[▶](#)[Back](#)[Close](#)[Full Screen / Esc](#)[Printer-friendly Version](#)[Interactive Discussion](#)

Vandaele, A. C., Hermans, C., Simon, P. C., Carleer, M., Colin, R., Fally, S., Merienne, M. F., Jenouvrier, A., and Coquart, B.: Measurements of the NO₂ absorption cross-section from 42 000 cm⁻¹ to 10 000 cm⁻¹ (238–1000 nm) at 220 K and 294 K, J. Quant. Spectrosc. Ra., 59, 171–184, doi:10.1016/S0022-4073(97)00168-4, 1998.

Washenfelder, R. A., Dubé, W. P., Wagner, N. L., and Brown, S. S.: Measurement of atmospheric ozone by cavity ring-down spectroscopy, Environ. Sci. Technol., in press, 2011.

Wayne, R. P., Barnes, I., Biggs, P., Burrows, J. P., Canosa-Mas, C. E., Hjorth, J., LeBras, G., Moortgat, G. K., Perner, D., Poulet, G., Restelli, G., and Sidebottom, H.: The nitrate radical: Physics, chemistry, and the atmosphere, Atmos. Environ. A-Gen., 25, 1–203, doi:10.1016/0960-1686(91)90192-A, 1991.

Yokelson, R. J., Burkholder, J. B., Fox, R. W., Talukdar, R. K., and Ravishankara, A. R.: Temperature-dependence of the NO₃ absorption-spectrum, J. Phys. Chem., 98, 13144–13150, 1994.

Zalicki, P. and Zare, R. N.: Cavity ring-down spectroscopy for quantitative absorption-measurements, J. Chem. Phys., 102, 2708–2717, doi:10.1063/1.468647, 1995.

Cavity ring-down instrument for N₂O₅, NO, NO₂ and O₃

N. L. Wagner et al.

[Title Page](#)

[Abstract](#)

[Introduction](#)

[Conclusions](#)

[References](#)

[Tables](#)

[Figures](#)

◀

▶

◀

▶

[Back](#)

[Close](#)

[Full Screen / Esc](#)

[Printer-friendly Version](#)

[Interactive Discussion](#)



Cavity ring-down instrument for N_2O_5 , NO , NO_2 and O_3

N. L. Wagner et al.

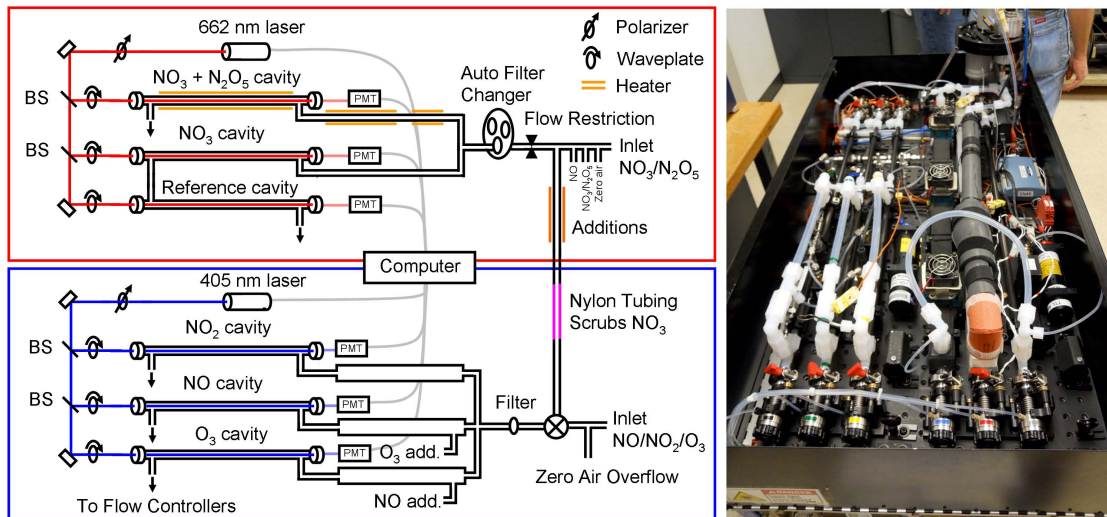


Fig. 1. Instrument schematic. The upper part framed in red shows the NO_3 and N_2O_5 measurement. The lower part framed in blue shows the NO , NO_2 and O_3 measurement. BS denotes a beamsplitter. A photo of the optical bench instrument is shown on the right.

[Title Page](#)

[Abstract](#)

[Introduction](#)

[Conclusions](#)

[References](#)

[Tables](#)

[Figures](#)

◀

▶

◀

▶

[Back](#)

[Close](#)

[Full Screen / Esc](#)

[Printer-friendly Version](#)

[Interactive Discussion](#)

Cavity ring-down instrument for N₂O₅, NO, NO₂ and O₃

N. L. Wagner et al.

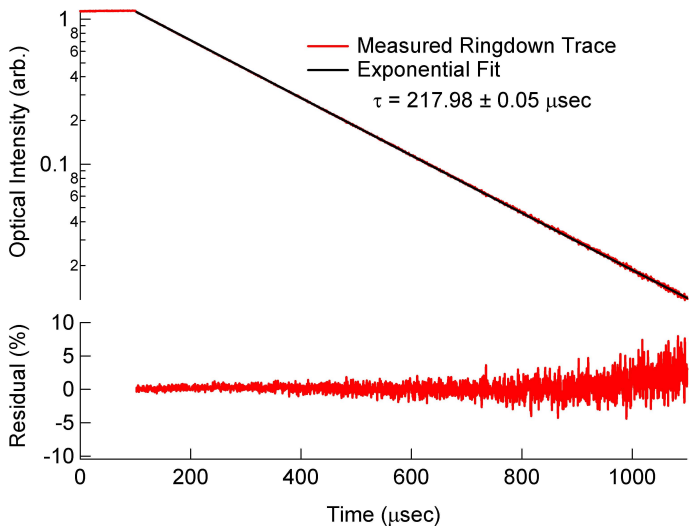


Fig. 2. Upper panel: ring-down trace from one of the 662 nm cavities, along with the fit to the ring-down trace. The lower panel shows the fit residual as a percentage of the fit.

Title Page

Abstract

Introduction

Conclusions

References

Tables

Figures



◀

1

Back

Close

Full Screen / Esc

[Printer-friendly Version](#)

Interactive Discussion



Cavity ring-down instrument for N₂O₅, NO, NO₂ and O₃

N. L. Wagner et al.

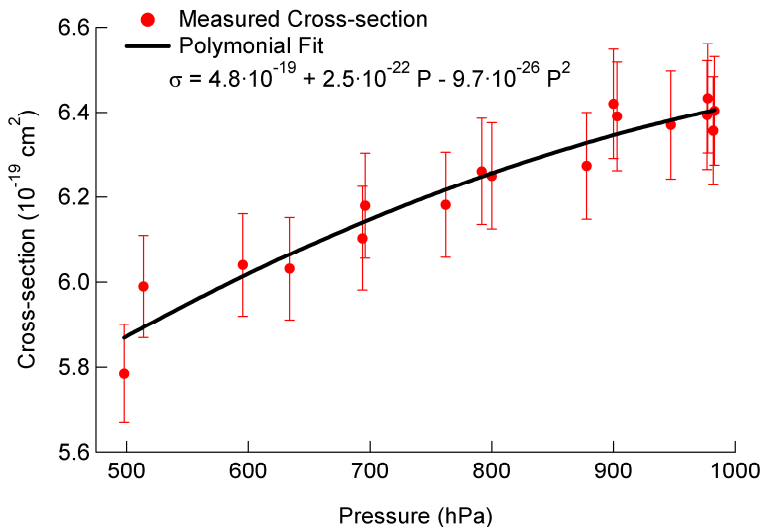


Fig. 3. Pressure dependence of the NO₂ cross-section at 405 nm. The pressure-dependent cross-section is parameterized by 3rd order polynomial and used for calculating NO₂ concentration during aircraft sampling at variable altitudes and cell pressures.

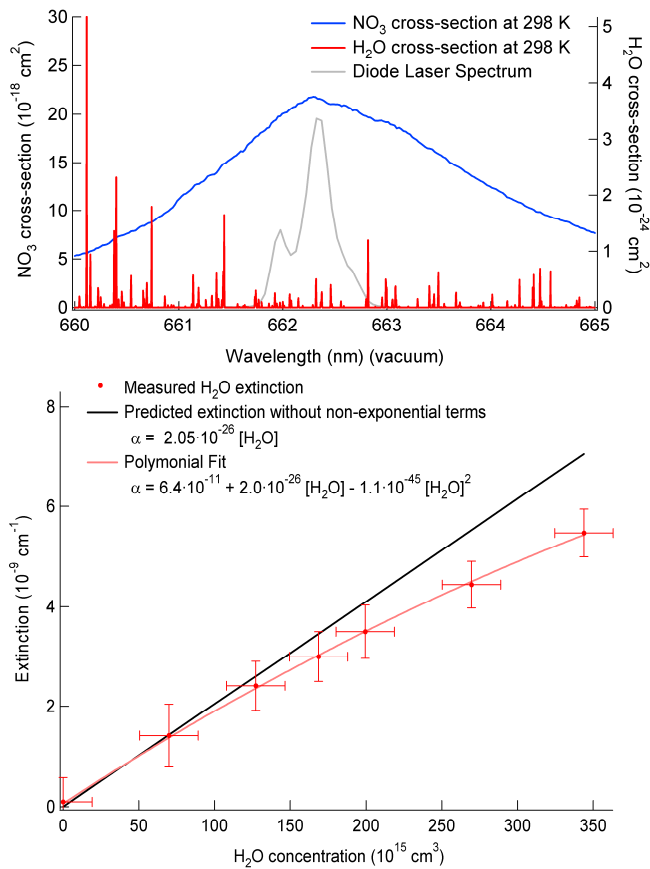


Fig. 4. The upper panel shows the NO_3 (blue) and water vapor (red) absorption spectrum around 662 nm. A typical laser spectrum is also shown. The lower panel shows the measured water sensitivity along with predicted sensitivity neglecting the non-exponential terms. The measured sensitivity is fit to a 3rd order polynomial and used to correct the field data.

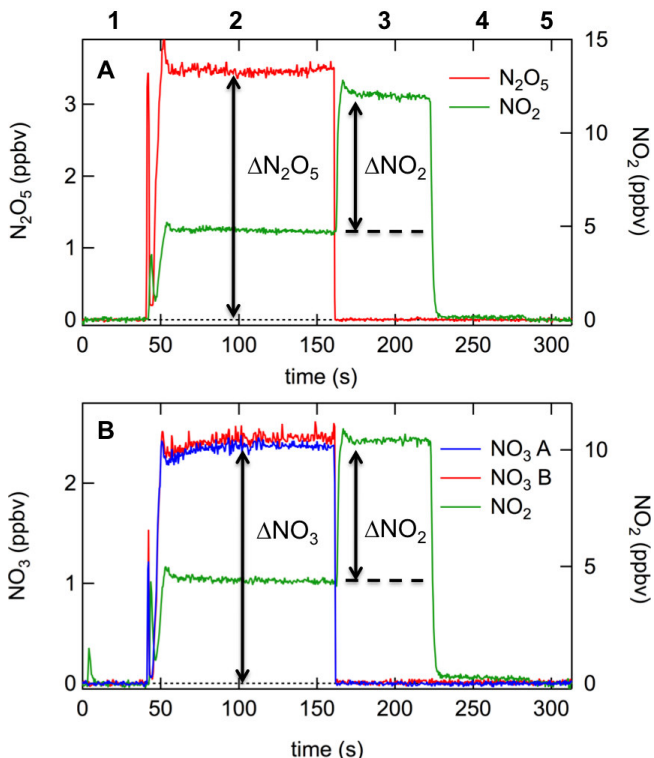


Fig. 5. Example calibration sequences for **(A)** N_2O_5 and **(B)** NO_3 . For the N_2O_5 calibration, the N_2O_5 source is added directly to the inlet, while for the NO_3 calibration it first passes through a heater to convert it primarily to NO_3 . The sequence of the calibration, indicated by the numbers across the top, includes (1) zero measurement; (2) addition of $\text{N}_2\text{O}_5/\text{NO}_3$ source; (3) titration of the $\text{NO}_3/\text{N}_2\text{O}_5$ source with excess NO to convert it to $2x \text{NO}_2$; (4) $\text{N}_2\text{O}_5/\text{NO}_3$ source switched off, NO titration on to determine NO_2 content of the added NO; and (5) NO titration turned off. The calibration is given by Eq. (3) and is effectively the ratio of $2\Delta(\text{N}_2\text{O}_5)/\Delta\text{NO}_2$ (or $2\Delta\text{NO}_3/\Delta\text{NO}_2$) marked in the figure, where ΔNO_2 is corrected for the small additional NO_2 in the added NO source given by the difference between (4) and (5) in the sequence above. For the data shown in the figure, the N_2O_5 calibration is 99%. The NO_3 calibrations factors are shown for the ambient channel (NO_3 in **A**) and the heated channel (NO_3 in **B**), and are 87% and 85%, respectively.

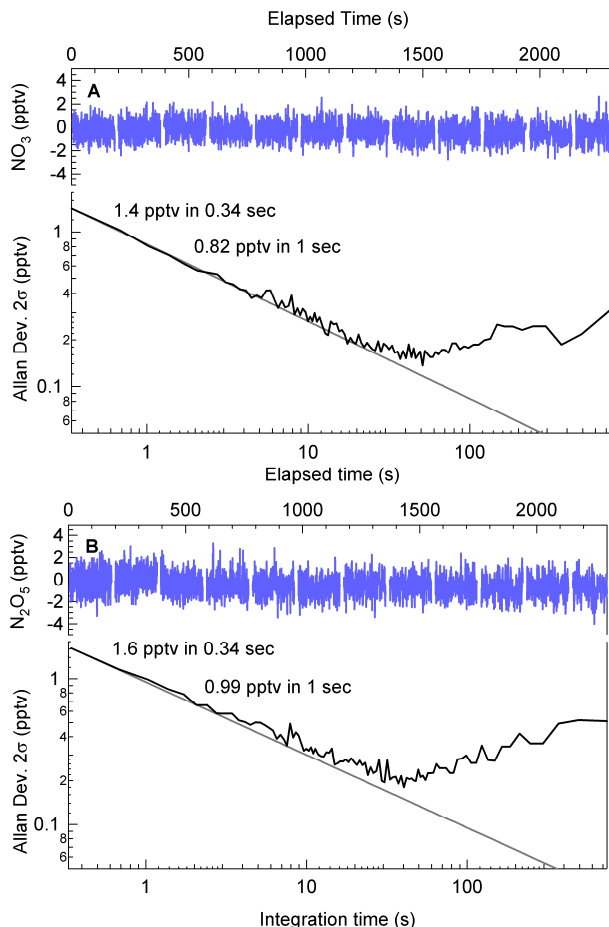


Fig. 6. Allan variance plots for the NO_3 (upper) and N_2O_5 (lower) measurements when sampling synthetic zero air. Both channels have a 2σ precision better than 1 pptv in 1 s.

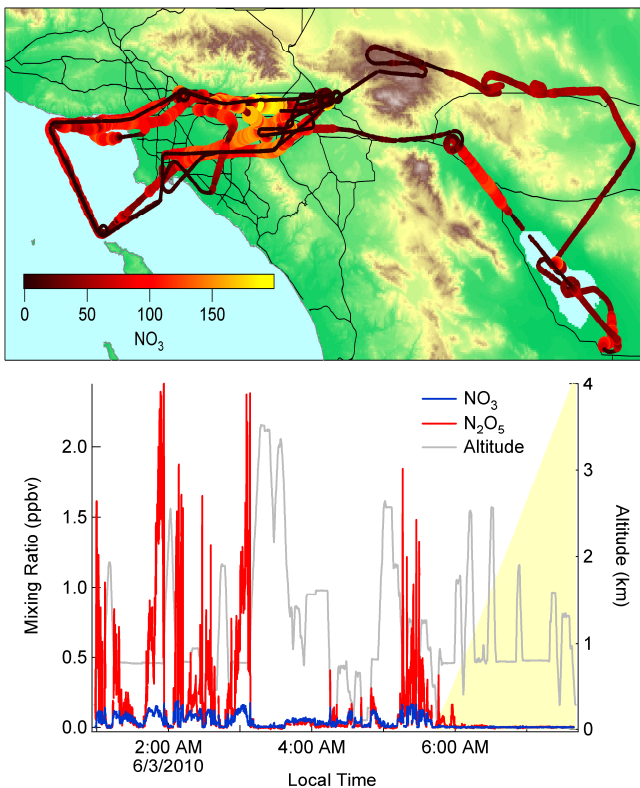


Fig. 7. Sample NO_3 and N_2O_5 data from the flight on 3 June 2010. The upper panel shows the flight track in the Los Angeles basin. The lower panel shows the NO_3 (blue) and N_2O_5 (red) mixing ratios measured during the flight along with the aircraft altitude in gray. The yellow background indicates the time of sunrise.

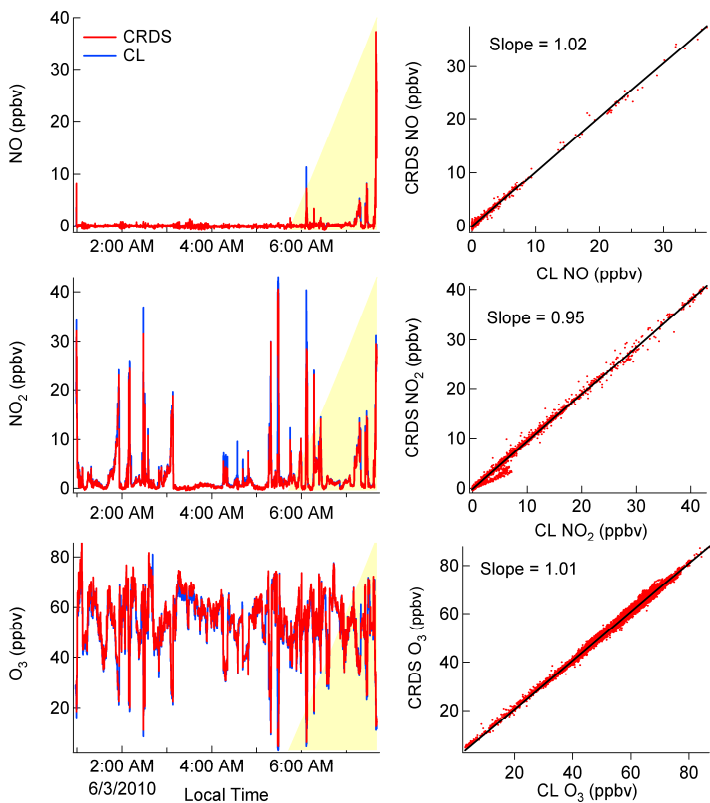


Fig. 8. The left panels show sample NO (blue), NO_2 (green) and O_3 (black) mixing ratio from both the CRDS instrument and the chemiluminescence (CL) measurements for the 3 June flight. The right panels show the correlations of the two measurements for each species. There was a small population of points on this flight for which there was a deviation on the NO_2 measurement, likely related to the zero measurement on one or the other instruments. These deviations were not observed on other CalNex flights.

Cavity ring-down instrument for N₂O₅, NO, NO₂ and O₃

N. L. Wagner et al.

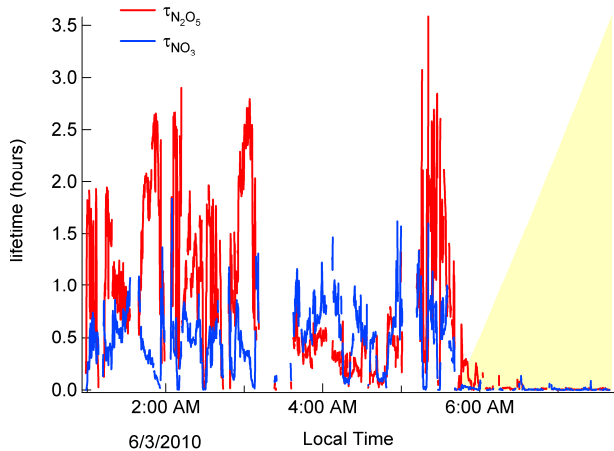


Fig. 9. The lifetimes of NO_3 (blue) and N_2O_5 (red) for the 3 June flight. The lifetimes were calculated using concentrations measured by a single instrument.

Title Page

Abstract

Introduction

Conclusions

References

Tables

Figures



Back

Close

Full Screen / Esc

[Printer-friendly Version](#)

Interactive Discussion

